Dalton Transactions

RSC Publishing

PAPER

View Article Online
View Journal | View Issue

Cite this: *Dalton Trans.*, 2013, **42**, 8498

Carbon monoxide release catalysed by electron transfer: electrochemical and spectroscopic investigations of [Re(bpy-R)(CO)$_4$](OTf) complexes relevant to CO_2 reduction†

Kyle A. Grice,‡ Nina X. Gu,‡ Matthew D. Sampson and Clifford P. Kubiak*

Received 6th March 2013,
Accepted 11th April 2013

DOI: 10.1039/c3dt50612f

www.rsc.org/dalton

[Re(bpy-*t*Bu)(CO)$_4$](OTf) (bpy-*t*Bu = 4,4′-di-*tert*-butyl-2,2′-bipyridine, OTf = trifluoromethanesulfonate) (**1**) and [Re(bpy)(CO)$_4$](OTf) (bpy = 2,2′-bipyridine) (**2**) were synthesized and studied as proposed intermediates in the electrocatalytic reduction of carbon dioxide (CO_2) by Re(bpy-R)(CO)$_3$X. Both compounds demonstrated increased current responses in cyclic voltammograms under CO_2. Complex **1** was also characterized by X-ray crystallography. Infrared-spectroelectrochemistry (IR-SEC) of **1** and **2** indicated that upon exposure of the cationic tetracarbonyl compounds to a reducing potential, a CO ligand is labilised and [Re(bpy-R)(CO)$_3$(CH$_3$CN)]$^+$ species are formed. This is proposed to occur *via* an electron-transfer-catalysed process wherein a catalytic amount of reduced species propagates a ligand exchange reaction. Addition of a catalytic amount of potassium intercalated graphite (KC_8), a chemical reductant, to a solution of **1** or **2** also yielded quantitative formation of [Re(bpy-R)(CO)$_3$(CH$_3$CN)]$^+$, which indicates that the CO loss is catalysed by electron transfer, and not the electrode itself.

Introduction

Current trends in worldwide energy consumption demonstrate a need for novel, sustainable fuel sources. Research into electrocatalytic carbon dioxide (CO_2) reduction aims to harness renewable energy to promote the conversion of CO_2 to starting materials for fuels. For example, reduction of CO_2 can generate carbon monoxide (CO), which can then be transformed into alkanes by the Fischer–Tropsch process.[1]

A variety of transition metal electrocatalysts for CO_2 reduction have been developed and studied.[2–5] Ideal catalysts would demonstrate high selectivity for CO_2 reduction to valuable products relative to proton reduction. The reduction of CO_2 is generally proton-coupled, but protons may also be directly reduced by an electrode or catalyst to produce hydrogen gas. In 1984, Lehn *et al*. reported that the Re(bpy)(CO)$_3$Cl (bpy = 2,2′-bipyridine) catalyst is effective at selectively reducing CO_2 to CO in the presence of water,[6] and further research found that replacement of the bipyridyl ligand with 4,4′-di-*tert*-butyl-2,2′-bipyridine (bpy-*t*Bu) significantly improves reaction rates for CO_2 reduction.[7] This modified system displays excellent selectivity toward carbon dioxide in the presence of proton sources, and protic additives increase activity for CO_2 reduction to CO.[8]

Our understanding of the mechanism of CO_2 reduction to CO by the Re(bpy-R)(CO)$_3$X system (R = H, Me, *t*Bu, X = halogen, OTf, or a neutral ligand with a non-coordinating anion) remains incomplete. Previous studies indicated that the complex undergoes a two-electron reduction and loses the X ligand to form a tricarbonyl anion (**A**), best described as a Re^0(bpy-R)$^{-1}$ species,[9] that enters the catalytic cycle (Scheme 1).[7] A potential mechanism invokes a carboxylate species (**B**) intermediate that is formed upon reaction of carbon dioxide with the anionic tricarbonyl species (**A**). The carboxylate species is protonated to form a carboxylic acid species (**C**), which could then react with a second proton to liberate water and produce a tetracarbonyl cationic intermediate (**D**) (Scheme 1).

It should be noted that the exact order of addition of protons, addition of electrons, and loss of product is not known, and further studies are needed to understand the intricacies of the mechanism. The intermediate species involved in

Department of Chemistry and Biochemistry, University of California San Diego, 9500 Gilman Drive MC 0358, La Jolla, California 92093, USA. E-mail: ckubiak@ucsd.edu; Fax: +1 858 534 5383; Tel: +1 858 822 2665

†Electronic supplementary information (ESI) available: Crystallographic data information for **1**, cyclic voltammetry scan rate studies of **1** and **2**, FT-IR and IR-SEC data for **1** and **2**, DFT-calculated LUMO of **1**, DFT-calculated SOMO of [Re(bpy-*t*Bu)(CO)$_4$]^0, and geometry optimized coordinates for computed structures are contained in the ESI. CCDC 917886 (**1**). For ESI and crystallographic data in CIF or other electronic format see DOI: 10.1039/c3dt50612f

‡These authors had equal contributions.

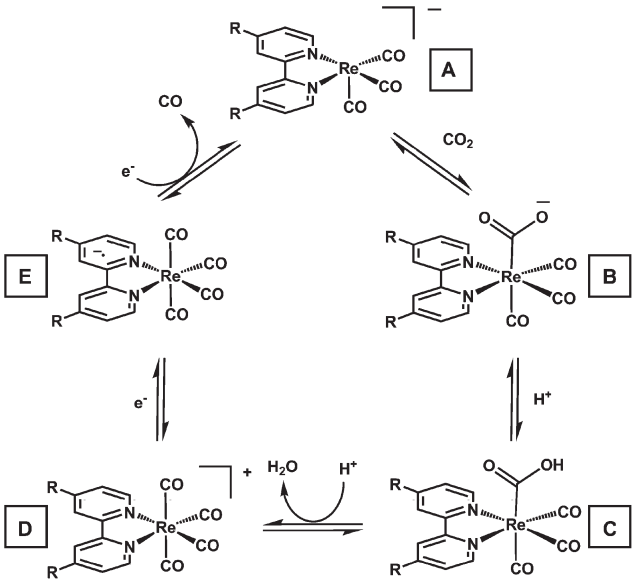

Scheme 1 A potential mechanism for the catalytic reduction of CO_2 to CO by Re(bpy-R)$(CO)_3$X species.

catalysis will likely depend on reduction potentials and pK_a's of the complexes compared to the applied potentials and pK_a's of the Brönsted acids available in solution. Turnover frequencies (TOFs) of the bpy-*t*Bu system greater than 250 s^{-1} have been reported.[7] One question in particular, then, is how the fourth CO ligand in **E** can be cleared sufficiently fast to create the site of coordinative unsaturation for the next CO_2 to bind.

In order to explore the proposed mechanism, we sought to discretely synthesize cationic tetracarbonyl complexes and study their role in the reduction of CO_2 through electrochemistry and Fourier Transform Infrared (FT-IR) spectroscopy. An improved understanding of the reactivity of these types of species should provide valuable insight into the catalytic cycle. In this report, we examine [Re(bpy-R)$(CO)_4$](OTf) (R = *t*Bu, **1**; H, **2**) species as they are stable complexes and are proposed intermediates in the catalytic cycle (**D** in Scheme 1). Their electrochemical and spectroscopic properties have been studied using electrochemistry, FT-IR spectroscopy, infrared-spectroelectrochemistry (IR-SEC), and chemical reduction. The results of this study are described below.

Results and discussion

Synthesis and characterization of [Re(bpy-R)$(CO)_4$](OTf) species

Complexes [Re(bpy-*t*Bu)$(CO)_4$](OTf) (**1**) and [Re(bpy)$(CO)_4$](OTf) (**2**) were synthesized similarly to a reported procedure for complex **2**,[10] and isolated as air-stable solids. Complex **1** was characterized by ^{1}H, ^{13}C, and ^{19}F NMR spectroscopy, as well as FT-IR spectroscopy and elemental analysis. A crystal of **1** suitable for X-ray crystallographic studies was obtained by vapor diffusion of hexane into a concentrated THF solution. The molecular structure of **1** was found to be consistent with all

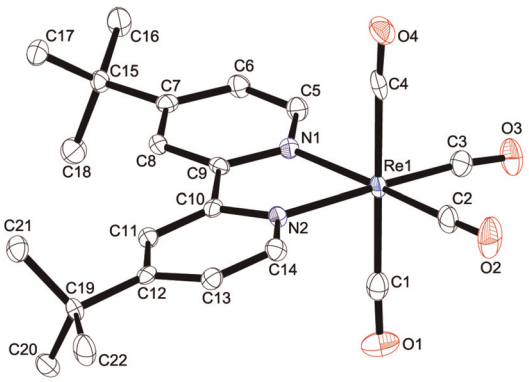

Fig. 1 Molecular structure of **1** with thermal ellipsoids shown at 50% probability. Hydrogen atoms and the trifluoromethanesulfonate anion are excluded for clarity.

Table 1 Selected bond lengths (Å) and angles (°) for **1**

Re–C1	1.984(4)
Re–C2	1.921(4)
Re–C3	1.933(4)
Re–C4	2.035(4)
Re–N1	2.163(3)
Re–N2	2.157(3)
C9–C10	1.473(5)
N1–C9	1.356(5)
N2–C10	1.355(5)
C1–O1	1.137(5)
C2–O2	1.144(5)
C3–O3	1.145(5)
C4–O4	1.112(5)
N1–Re–N2	74.8(1)
N2–Re–C2	98.5(1)
C2–Re–C3	87.6(2)
C3–Re–N1	99.3(1)
C1–Re–C4	178.8(2)

other characterization (Fig. 1, with pertinent bond lengths and angles listed in Table 1). The structure of **1** is very similar to the reported structure for **2**,[11] with one notable feature being a large difference in length of the two axial Re–CO bonds, although this is possibly due to a crystal packing effect. The FT-IR spectrum of **1** in the ν(CO) region is similar to **2**, but shifted slightly to lower wavenumbers, as is expected from the electron-donating *t*Bu groups on complex **1** (Table 2).

Electrochemistry of 1 and 2

The electrochemistry of complexes **1** and **2** was studied using a glassy carbon (GC) working electrode in acetonitrile with 0.1 M tetrabutylammonium hexafluorophosphate (TBAH). Both complexes exhibit cyclic voltammograms (CVs) in which a small, irreversible wave is followed by two larger quasi-reversible waves (Fig. 2 for **1**, Fig. S1 in the ESI† for **2**, data summarized

Table 2 FT-IR data for complexes **1** and **2** in acetonitrile

Complex	ν(CO) (cm^{-1})
1	2123, 2026, 2006, 1964
2	2125, 2029, 2008, 1966

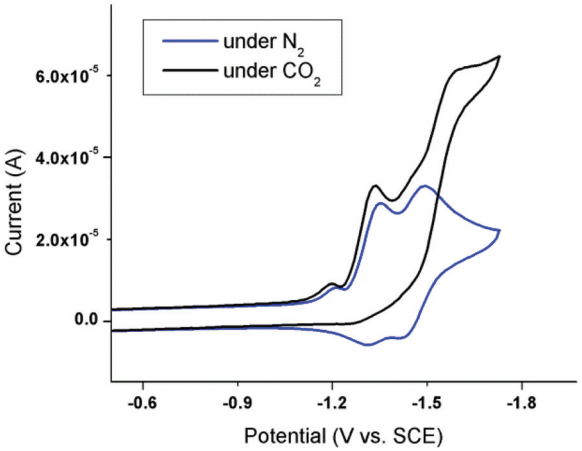

Fig. 2 Cyclic voltammograms of **1** (1 mM) under nitrogen (blue) and carbon dioxide (black). Voltammograms were taken at 100 mV s^{-1} in a solution of 0.1 M TBAH in acetonitrile with a glassy carbon working electrode, a Ag wire pseudo-reference electrode and a Pt counter electrode. Ferrocene was added as an internal reference.

Table 3 Reduction potentials (V *vs.* SCE)

Complex	Under N_2	Under CO_2
1	-1.23^a, −1.37, −1.51	-1.21^a, −1.35, -1.62^b
2	-1.15^a, −1.27, −1.42	-1.15^a, −1.26, -1.53^b

All potentials measured as E_{peak}. [a] Small, irreversible peak. [b] Catalytic increase in current.

in Table 3). The first reduction potential for **2** is consistent with a previously reported value in acetonitrile, which was also found to be irreversible.[12] Scan rate studies of complexes **1** and **2** show that these 3 reductions are related to freely diffusing species and also that each of the waves relate to 1 e^- events (Fig. S2–S5 in the ESI†).[13]

Under CO_2, current increase and loss of reversibility is observed at the most negative of the large waves for both **1** and **2**, consistent with catalytic reduction of CO_2. It should be noted that the potentials at which catalysis begins are more positive than those of the corresponding Re(bpy-R)$(CO)_3$Cl species by 330–340 mV.[7] The catalysis observed for complex **1** also showed a much lower i_{cat}/i_p value (1.9) compared to the Re(bpy-*t*Bu)$(CO)_3$Cl complex (18.3).[7]

Infrared-spectroelectrochemistry (IR-SEC)

The IR-SEC of complexes **1** and **2** were studied at a platinum electrode in acetonitrile with 0.1 M TBAH under a N_2 atmosphere in order to better understand the electrochemical behavior seen in the cyclic voltammograms. As reducing potentials are applied to a solution of **1**, the stretches assigned to the ν(CO) bands for complex **1** begin to disappear with a concomitant growth of new signals for a complex (**3**) with a sharp band at 2041 cm^{-1} and a broader band at 1936 cm^{-1} (Fig. 3). This pattern is indicative of a tricarbonyl species.[7] Similarly, when reducing potentials are applied to complex **2**, the first new

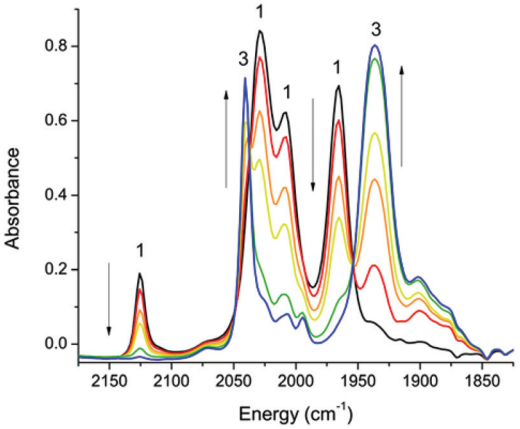

Fig. 3 First reduction of **1** (4 mM) by IR-SEC in 0.1 M TBAH in acetonitrile to yield **3** by electrode-catalysed substitution.

species (**4**) that appears in the FT-IR spectrum has a sharp ν(CO) band at 2043 cm^{-1} and a broader band at 1939 cm^{-1} (Fig. S6†). These ν(CO) bands for **3** and **4** are consistent with a Re^I cation, and match well with the reported IR spectra of $[Re(bpy\text{-}tBu)(CO)_3(CH_3CN)]^+$ and $[Re(bpy)(CO)_3(CH_3CN)]^+$.[8,14] From this data, we interpret complexes **3** and **4** to be $[Re(bpy\text{-}R)(CO)_3(CH_3CN)]^+$ complexes (R = *t*Bu (**3**), H (**4**)). It should be noted that formation of **3** and **4** from **1** and **2** are not reductions, but rather ligand substitution reactions.

As more reducing potentials are applied to complexes **3** and **4**, two new species subsequently appear for each of the complexes (Fig. S5 and S6 and Tables S7 and S8 in the ESI†). The ν(CO) bands for these species do not match with previously observed ν(CO) bands for $[Re(bpy\text{-}R)(CO)_3]^0$ or $[Re(bpy\text{-}R)(CO)_3]^{-1}$ complexes, which were observed in the IR-SEC of Re(bpy-R)$(CO)_3$Cl.[7] These further reduced species are assigned as $[Re(bpy\text{-}R)(CO)_3(CH_3CN)]^0$ (**5** and **6**) and $[Re(bpy\text{-}R)(CO)_3(CH_3CN)]^{-1}$ (**7** and **8**) based on comparison with previous IR data obtained for $[Re(bpy)(CO)_3(CH_3CN)]^+$ in mixed THF–CH_3CN solvent,[15] and IR data for $[Re(bpy)(CO)_3(n\text{-}PrCN)]^{0/-1}$ in *n*-PrCN.[16] This assignment is further supported by the fact that the second and third reductions observed in the electrochemistry of **1** and **2** are in reasonable agreement with previously reported numbers for the first and second reductions of $[Re(bpy\text{-}R)(CO)_3(CH_3CN)]^+$ in CH_3CN.[8,12]

Carbon monoxide substitution catalysed by chemical reduction

Controlled potential electrolysis of 5 mM solutions **1** at potentials more negative than the first reduction lead to consumption of 26 mol% of coulombs and complex **3** is the only species observed in the FT-IR spectrum of the resulting solution, indicating that the ligand substitution was indeed catalytic in nature. However, determination of the exact number of coulombs necessary for catalysis is hampered by various factors, such as capacitive current and the ability of the counter electrode to generate oxidized species in solution that could interact with the working electrode or the reduced

$[Re(bpy\text{-}R)(CO)_4]^0$ complexes. Therefore, the 26 mol% of electrons should be considered an overestimation.

In order to determine if the electron-transfer-catalysed CO loss from **1** or **2** was due to the presence of the electrodes in the electrochemical cells, or due to an inherent characteristic of the compounds, chemical reduction experiments were performed. When solutions of **1** or **2** in acetonitrile were exposed to sub-stoichiometric amounts of KC_8 (0.10–0.16 equiv.), conversion to the corresponding $[Re(bpy\text{-}R)(CO)_3(CH_3CN)]^+$ complexes was observed, as determined by FT-IR spectroscopy. Notably, conversion was rapid (within minutes) and complete when 0.1 M TBAH solutions of **1** or **2** were used (Fig. S9 and S10 in ESI†). Without TBAH supporting electrolyte, the substitution reactions did not reach completion (Fig. S11 and S12 in ESI†). This is likely due to the ability of the electrolyte to facilitate the many charge transfer events necessary in the electron-transfer-catalysed ligand substitution reaction.

Electron-transfer-catalysed ligand substitution

The fact that a Re^I cation (**3** and **4**) is formed from formal reduction of a Re^I cation (**1** and **2**) is very intriguing. Allowing complex **1** or **2** to stand in acetonitrile at room temperature does not lead to substitution as determined by FT-IR experiments, which indicates that the ligand exchange process requires catalytic reduction to proceed. There is precedent for this reduction-catalysed ligand substitution at group 7 metals,[17] as well as at a variety of metal carbonyls,[18] including group 6 $M(bpy)(CO)_4$ complexes.[19,20] A significant difference between the group 6 $M(bpy)(CO)_4$ complexes and complexes **1** and **2** is that a reduced $[M(bpy)(CO)_4]^-$ species is stable and can be characterised by FT-IR, whereas we have found no spectroscopic evidence for reduced $[Re(bpy\text{-}R)(CO)_4]^0$ complexes. These $[Re(bpy\text{-}R)(CO)_4]^0$ complexes are likely transient intermediates in the electron-transfer-catalysed ligand substitution of **1** and **2**. If a small amount of $[Re(bpy\text{-}R)(CO)_4]^0$ is formed, ligand exchange can occur with solvent, leading to $[Re(bpy\text{-}R)(CO)_3(CH_3CN)]^0$, which undergoes electron transfer with more starting material (**1** or **2**), resulting in the catalytic cycle that is shown in Scheme 2.

The electrode-catalysed ligand substitution is likely the reason the peak current of the first reduction observed for **1** and **2** is small compared to the subsequent reductions in the cyclic voltammograms at 100 mV s^{-1}. At higher scan rates, the first reduction of **1** and **2** merges with the second reduction and becomes a reversible event, whereas the most negative reduction becomes irreversible. This is because at these fast scan rates (approaching 5 V s^{-1}), the $[Re(bpy\text{-}R)(CO)_4]^0$ species are stable, and therefore the reductions of $[Re(bpy\text{-}R)(CO)_4]^+$ are reversible and of the expected current. The reduction of $[Re(bpy\text{-}R)(CO)_4]^0$ liberates CO irreversibly, which causes the final reduction to become more irreversible at faster scan rates.

In the reductions of $Re(bpy\text{-}R)(CO)_3Cl$ species, the first reduction is primarily bpy-based.[7] We were curious if this were also true for **1** and **2**. We performed density functional theory (DFT) calculations on both **1** and the mono-reduced species $[Re(bpy\text{-}t\text{Bu})(CO)_4]^0$. The lowest unoccupied molecular orbital (LUMO) of **1** and the singly occupied molecular orbital (SOMO) of $[Re(bpy\text{-}t\text{Bu})(CO)_4]^0$ were found to be primarily bpy-based (see Fig. S13 and S14 in the ESI†). The labilisation of a Re–CO bond upon reduction of the bpy ligand has been explained by donation of spin density from the occupied π^* orbitals of the reduced bpy ligand to the *cis* carbonyls.[14,21]

Relevance to CO_2 reduction mechanism

This electrode-catalysed ligand substitution reaction that appears to be very facile for both **1** and **2** is likely an important product-releasing step in CO_2 reduction by $Re(bpy\text{-}R)(CO)_3X$ catalysts. It is notable that the reductions of **1** and **2** occur at potentials much more positive than potentials employed in CO_2 reduction catalysis by $Re(bpy\text{-}R)(CO)_3X$ catalysts.[7,8] This means that if a $[Re(bpy\text{-}R)(CO)_4]^+$ species is formed in the catalytic cycle, it would be reduced and release CO prior to accessing the catalytically-active, anionic species $[Re(bpy\text{-}R)(CO)_3]^{-1}$. Clearly, product loss is not a bottleneck to catalysis with the $Re(bpy\text{-}R)(CO)_3X$ system. Further studies are needed to fully elucidate the complete catalytic mechanism for these highly active and selective catalysts.

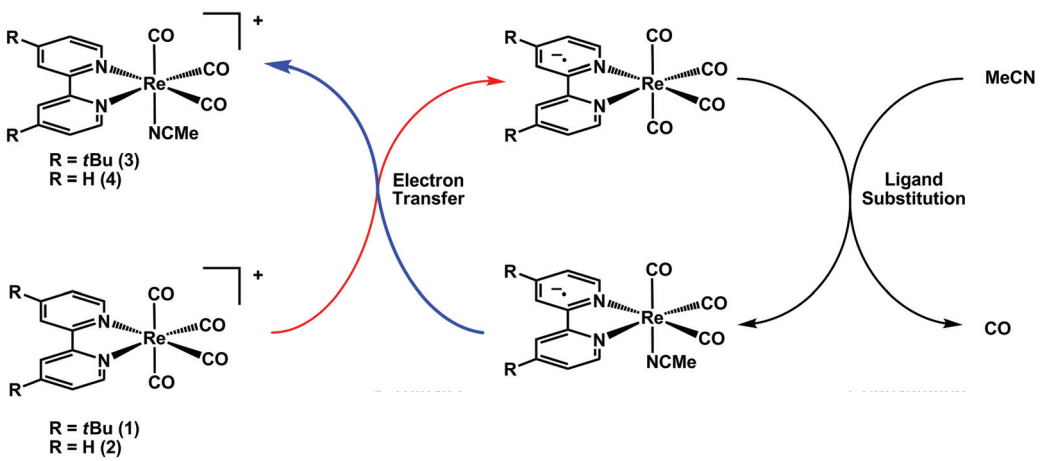

Scheme 2 Electron-transfer-catalysed ligand substitution of **1** and **2**.

Conclusions

The rhenium tetracarbonyl cations [Re(bpy-R)(CO)$_4$](OTf) (R = *t*Bu (**1**), H (**2**)) have been synthesized and characterised. Complex **1** was characterized by X-ray crystallography. Electrochemical, IR-SEC, and chemical reduction studies of **1** and **2** have shown that these species undergo an electron-transfer-catalysed ligand substitution reaction in CH_3CN, leading to [Re(bpy-R)(CO)$_3$(CH_3CN)]$^+$ complexes (**3** and **4**). This occurs at potentials that are *ca.* 0.5 V more positive than the potentials at which catalysis occurs with Re(bpy-R)(CO)$_3$Cl, indicating that product elimination is extremely facile in CO_2 reduction catalysis. This catalytic CO-release by sub-stoichiometric electron transfer may also find use in the development of targeted delivery of CO for medical and other applications.[22]

Experimental section

General considerations

Manipulations were performed using standard Schlenk and glove box techniques. Re(CO)$_5$Cl, 4,4′-di-*tert*-butyl-2,2′-bipyridine and 2,2′-bipyridine were obtained from Aldrich, and silver trifluoromethanesulfonate (AgOTf) was obtained from Alfa Aesar. These reagents were used without further purification. Tetrabutylammonium hexafluorophosphate (TBAH) was recrystallized from methanol and dried under vacuum. Potassium intercalated graphite (KC_8) was synthesized according to a literature procedure.[23] Dichloromethane (DCM), acetonitrile (CH_3CN), pentane, and tetrahydrofuran (THF) were dried over basic alumina with a custom dry solvent system. NMR spectra were obtained on a Varian 300 MHz, a Jeol 500 MHz, and a Varian 500 MHz spectrometer at 298 K. ^{1}H and ^{13}C NMR data are referenced to residual solvent peaks and reported in ppm downfield of TMS (δ = 0 ppm). ^{19}F NMR data are referenced to an external standard (trifluoroacetic acid, δ = −76.55 ppm) and reported downfield of trichlorofluoromethane (δ = 0 ppm). Infrared spectra were obtained on a Thermo Nicolet 6700. Elemental analysis was performed by Midwest Microlab, LLC, Indianapolis for C, H, N composition.

Synthesis [Re(bpy-R)(CO)$_4$](OTf) (R = *t*Bu, 1; H, 2)

Complexes **1** and **2** were synthesized according to literature methods for **2**.[10] Re(CO)$_5$Cl (0.400 g, 1.1 mmol) was dissolved in 80 mL DCM in a round bottom flask. AgOTf (0.300 g, 1.2 mmol) dissolved in 20 mL DCM was added to the flask. The reaction mixture was left stirring at room temperature in the dark under nitrogen for 21 h. AgCl precipitate was filtered off and washed with 30 mL DCM. The appropriate bipyridine ligand was added to the filtrate, bpy-*t*Bu (0.329 g, 1.2 mmol) for **1** or bpy (0.190 g, 1.2 mmol) for **2**, and the reaction was allowed to stir for 8 h in the dark under a nitrogen atmosphere. The reaction mixture was concentrated *in vacuo* to 20 mL, and 100 mL of hexanes was added to precipitate a yellow solid that was subsequently removed by filtration and dried. A typical overall yield of 55% was obtained for complexes **1** and **2**.

Characterization for complex **1**: ^{1}H NMR ($CDCl_3$, 500 MHz): δ = 1.50 (s, 9H), 7.67 (dd, J = 6.0, 1.9 Hz, 2H), 8.54 (d, J = 2.0 Hz, 2H), 8.81 (d, J = 5.9 Hz, 2H). ^{13}C NMR ($CDCl_3$, 125.7 MHz): δ = 30.28, 36.35, 123.14, 126.10, 153.37, 156.64, 167.00, 182.52, 187.75. ^{19}F NMR ($CDCl_3$, 282.32 MHz): δ = −77.29. IR (THF) ν(CO): 2120 cm^{-1}, 2028 cm^{-1}, 2008 cm^{-1}, 1957 cm^{-1}. IR (CH_3CN) ν(CO): 2123 cm^{-1}, 2026 cm^{-1}, 2006 cm^{-1}, 1964 cm^{-1}. Anal. Calcd for **1**, $C_{23}H_{24}F_3N_2O_7ReS$: C, 38.60; H, 3.38; N, 3.91. Found: C, 38.53; H, 3.39; N, 4.04.

Characterization for complex **2**: ^{1}H NMR ($CDCl_3$, 500 MHz): δ = 7.79–7.70 (m, 2H), 8.42 (t, J = 7.9 Hz, 2H), 8.93 (d, J = 5.5 Hz, 2H), 9.02 (d, J = 8.3 Hz, 2H). ^{13}C NMR ($CDCl_3$, 125.7 MHz): δ = 126.90, 129.07, 142.41, 153.84, 156.57, 182.50, 187.22. ^{19}F NMR ($CDCl_3$, 282.32 MHz): δ = −77.23. IR (THF) ν(CO): 2121 cm^{-1}, 2026 cm^{-1}, 2003 cm^{-1}, 1961 cm^{-1}. IR (CH_3CN) ν(CO): 2125 cm^{-1}, 2029 cm^{-1}, 2008 cm^{-1}, 1966 cm^{-1}. Spectral data for **2** matched literature reports.[10]

Electrochemistry

Electrochemical studies were performed with a BAS Epsilon or a BAS CV50 potentiostat. The cell was composed of a 3 mm diameter glassy carbon working electrode, Ag wire pseudo-reference and Pt wire counter electrode. Ferrocene (Fc) was added as an internal reference. All experiments were run in 0.1 M TBAH as supporting electrolyte in CH_3CN and N_2 or CO_2 was used to purge the cell before each voltammogram. Decamethylferrocene (Fc*) was used as an internal reference for scan rate studies.

Infrared-spectroelectrochemistry (IR-SEC)

The design and setup of the IR spectroelectrochemical cell has been previously described in the literature.[24] A platinum working electrode was used with a silver pseudo-reference electrode and a platinum counter electrode. All experiments were performed with CH_3CN solution with 0.1 M TBAH, and all samples were prepared under nitrogen in a glove box. Blank 0.1 M TBAH CH_3CN solutions were prepared and used for solvent subtraction. Spectra were obtained on a Bruker Equinox 55 spectrometer and a Pine Instrument Company Model AFCBP1 bipotentiostat was used to reduce the samples. Samples of **1** or **2** were prepared in concentrations of 1–5 mM for IR-SEC.

Chemical reductions of 1 and 2 with KC_8

Acetonitrile solutions of **1** or **2** (50 mM, 1–2 mL) were made with or without 0.1 M TBAH. KC_8 (0.10–0.16 equiv.) was added, the solutions were agitated and the solid was allowed to settle. FT-IR spectra were taken within 10 minutes of mixing. 50 mM solutions of **1** or **2** and 0.1 M TBAH in acetonitrile without KC_8 were taken to obtain initial FT-IR spectra.

X-ray crystallography

Single crystal X-ray diffraction studies were carried out on a Bruker PHOTON 100 CMOS diffractometer equipped with Mo Kα radiation (λ = 0.71073 Å). The crystals were mounted on

a Cryoloop with Paratone oil, and data were collected under a nitrogen gas stream at 100(2) K using ω and ϕ scans. Data were integrated using the Bruker SAINT software program and scaled using the SADABS software program. Solution by direct methods (SHELXS) produced a complete phasing model consistent with the proposed structure. All non-hydrogen atoms were refined anisotropically by full-matrix least-squares (SHELXL-97).[25] All hydrogen atoms were placed using a riding model. Their positions were constrained relative to their parent atom using the appropriate HFIX command in SHELXL-97. Crystallographic data are summarized in Table S1.†

DFT calculations

Density functional theory (DFT) calculations were performed with the Amsterdam density functional (ADF) program suite (version 2007.01).[26–28] The triple-ζ Slater-type orbital TZ2P basis set was utilized without frozen cores for all atoms. Relativistic effects were included *via* the zeroth-order regular approximation (ZORA).[29,30] The BP86 functional and the local density approximation (LDA) of Vosko, Wilk, and Nusair (VWN)[31] was coupled with the generalized gradient approximation (GGA) corrections described by Becke[32] and Perdew[33,34] for electron exchange and correlation, respectively. Frequency calculations were performed to verify that the optimized geometries were at minima. Geometry optimized *xyz* coordinates and a sample input file are included in the ESI.†

Acknowledgements

This work was supported by the Air Force Office of Scientific Research through the MURI program under AFOSR Award FA9550-10-1-0572. N. X. Gu's summer undergraduate research at UCSD was made possible by the 2012 Amgen Scholars Program, supported by the Amgen Foundation. Dr. Eric Benson, Dr. Curtis Moore, and Professor Arnold Rheingold are acknowledged for assistance with crystallography. Gabriel Canzi and Jane Hendersen are thanked for assistance with IR-SEC experiments.

Notes and references

1 M. E. Dry, *Catal. Today*, 2002, **71**, 227–241.
2 E. E. Benson, C. P. Kubiak, A. J. Sathrum and J. M. Smieja, *Chem. Soc. Rev.*, 2009, **38**, 89–99.
3 J.-M. Savéant, *Chem. Rev.*, 2008, **108**, 2348–2378.
4 C. D. Windle and R. N. Perutz, *Coord. Chem. Rev.*, 2012, **256**, 2562–2570.
5 C. Costentin, M. Robert and J.-M. Saveant, *Chem. Soc. Rev.*, 2013, **42**, 2423–2436.
6 J. Hawecker, J. M. Lehn and R. Ziessel, *J. Chem. Soc., Chem. Commun.*, 1984, 328–330.
7 J. M. Smieja and C. P. Kubiak, *Inorg. Chem.*, 2010, **49**, 9283–9289.
8 J. M. Smieja, E. E. Benson, B. Kumar, K. A. Grice, C. S. Seu, A. J. M. Miller, J. M. Mayer and C. P. Kubiak, *Proc. Natl. Acad. Sci. U. S. A.*, 2012, **109**, 15646–15650.
9 E. E. Benson, M. D. Sampson, K. A. Grice, J. M. Smieja, J. D. Froehlich, D. Friebel, J. A. Keith, E. A. Carter, A. Nilsson and C. P. Kubiak, *Angew. Chem., Int. Ed.*, 2013, **52**, 4841–4844.
10 R. J. Shaver and D. P. Rillema, *Inorg. Chem.*, 1992, **31**, 4101–4107.
11 T. Scheiring, W. Kaim and J. Fiedler, *J. Organomet. Chem.*, 2000, **598**, 136–141.
12 T. Scheiring, A. Klein and W. Kaim, *J. Chem. Soc., Perkin Trans. 2*, 1997, 2569–2572.
13 J. Wang, *Analytical Electrochemistry*, John Wiley & Sons, 2006.
14 A. Klein, C. Vogler and W. Kaim, *Organometallics*, 1996, **15**, 236–244.
15 F. P. A. Johnson, M. W. George, F. Hartl and J. J. Turner, *Organometallics*, 1996, **15**, 3374–3387.
16 J. W. M. Van Outersterp, F. Hartl and D. J. Stufkens, *Organometallics*, 1995, **14**, 3303–3310.
17 G. J. Stor, F. Hartl, J. W. M. van Outersterp and D. J. Stufkens, *Organometallics*, 1995, **14**, 1115–1131.
18 N. J. Coville, in *Organometallic Radical Processes*, ed. W. C. Trogler, Elsevier, Amsterdam, 1990, pp. 108–141.
19 D. Miholová and A. A. Vlček, *J. Organomet. Chem.*, 1985, **279**, 317–326.
20 B. Olbrich-Deussner and W. Kaim, *J. Organomet. Chem.*, 1988, **340**, 71–91.
21 W. Kaim, in *Journal of Organometallic Chemistry Library*, ed. W. C. Trogler, Elsevier, Amsterdam, 1990, pp. 173–200.
22 R. Alberto and R. Motterlini, *Dalton Trans.*, 2007, 651–1660.
23 M. A. Schwindt, T. Lejon and L. S. Hegedus, *Organometallics*, 1990, **9**, 2814–2819.
24 I. S. Zavarine and C. P. Kubiak, *J. Electroanal. Chem.*, 2001, **495**, 106–109.
25 G. Sheldrick, *Acta Crystallogr., Sect. A: Fundam. Crystallogr*, 2008, **64**, 112–122.
26 C. Fonseca Guerra, J. G. Snijders, G. te Velde and E. J. Baerends, *Theor. Chem. Acc.*, 1998, **99**, 391–403.
27 G. te Velde, F. M. Bickelhaupt, E. J. Baerends, C. Fonseca Guerra, S. J. A. van Gisbergen, J. G. Snijders and T. Ziegler, *J. Comput. Chem.*, 2001, **22**, 931–967.
28 ADF 2007.01, *Theoretical Chemistry*, Vrije Universiteit, Amsterdam, The Netherlands, 2007, www.scm.com.
29 E. van Lenthe, E. J. Baerends and J. G. Snijders, *J. Chem. Phys.*, 1993, **99**, 4597–4610.
30 E. v. Lenthe, J. G. Snijders and E. J. Baerends, *J. Chem. Phys.*, 1996, **105**, 6505–6516.
31 S. H. Vosko, L. Wilk and M. Nusair, *Can. J. Phys.*, 1980, **58**, 1200–1211.
32 A. D. Becke, *Phys. Rev. B: Condens. Matter*, 1988, **38**, 3098–3100.
33 J. P. Perdew, *Phys. Rev. B: Condens. Matter*, 1986, **33**, 8822–8824.
34 J. P. Perdew, *Phys. Rev. B: Condens. Matter*, 1986, **34**, 7406–7406.